doi:10.1093/brain/awr322 Brain 2012: 135; 72–87 | 72

BRAIN
A JOURNAL OF NEUROLOGY

A rat model of Charcot–Marie–Tooth disease 1A recapitulates disease variability and supplies biomarkers of axonal loss in patients

Robert Fledrich,[1] Beate Schlotter-Weigel,[2] Tuuli J. Schnizer,[1] Sven P. Wichert,[1] Ruth M. Stassart,[1] Gerd Meyer zu Hörste,[3] Axel Klink,[1] Bernhard G. Weiss,[1] Uwe Haag,[4] Maggie C. Walter,[2] Bernd Rautenstrauss,[5] Walter Paulus,[6] Moritz J. Rossner[1] and Michael W. Sereda[1,6]

1 Department of Neurogenetics, Max-Planck-Institute of Experimental Medicine, Hermann-Rein-Str. 3, D-37075 Göttingen, Germany
2 Friedrich-Baur-Institut, Neurologische Klinik und Poliklinik, Labor für Molekulare Myologie, Ludwig-Maximilians-Universität, Ziemssenstr. 1, D-80336 München, Germany
3 Department of Neurology, Heinrich-Heine-University, Moorenstraße 5, D-40225 Düsseldorf, Germany
4 HaaPACS GmbH, Bahnhofstr. 19c, D-69198 Schriesheim, Germany
5 Medizinisch Genetisches Zentrum (MGZ), Bayerstraße 3-5, D-80335 München, Germany
6 Department of Clinical Neurophysiology, University of Göttingen, Robert-Koch Str. 40, D-37075 Göttingen, Germany

Correspondence to: Dr Michael W. Sereda,
Research Group 'Molecular and Translational Neurology',
Department of Neurogenetics,
Max-Planck-Institute of Experimental Medicine,
Hermann-Rein-Str. 3,
D-37075 Göttingen, Germany
E-mail: sereda@em.mpg.de

Charcot–Marie–Tooth disease is the most common inherited neuropathy and a duplication of the *peripheral myelin protein 22* gene causes the most frequent subform Charcot–Marie–Tooth 1A. Patients develop a slowly progressive dysmyelinating and demyelinating peripheral neuropathy and distally pronounced muscle atrophy. The amount of axonal loss determines disease severity. Although patients share an identical monogenetic defect, the disease progression is strikingly variable and the impending disease course can not be predicted in individual patients. Despite promising experimental data, recent therapy trials have failed. Established clinical outcome measures are thought to be too insensitive to detect amelioration within trials. Surrogate biomarkers of disease severity in Charcot–Marie–Tooth 1A are thus urgently needed. Peripheral myelin protein 22 transgenic rats harbouring additional copies of the *peripheral myelin protein 22* gene ('Charcot–Marie–Tooth rats'), which were kept on an outbred background mimic disease hallmarks and phenocopy the variable disease severity of patients with Charcot–Marie–Tooth 1A. Hence, we used the Charcot–Marie–Tooth rat to dissect prospective and surrogate markers of disease severity derived from sciatic nerve and skin tissue messenger RNA extracts. Gene set enrichment analysis of sciatic nerve transcriptomes revealed that dysregulation of lipid metabolism associated genes such as *peroxisome proliferator-activated receptor gamma* constitutes a modifier of present and future disease severity. Importantly, we directly validated disease severity markers from the Charcot–Marie–Tooth rats in 46 patients with Charcot–Marie–Tooth 1A. Our data suggest that the combination of age and cutaneous messenger RNA levels of *glutathione S-transferase theta 2* and *cathepsin A* composes a strong indicator of disease severity in patients with Charcot–Marie–Tooth 1A, as quantified by the Charcot–Marie–Tooth Neuropathy Score. This translational approach, utilizing a transgenic animal model, demonstrates that transcriptional analysis of skin biopsy is suitable to identify biomarkers of Charcot–Marie–Tooth 1A.

Received June 30, 2011. Revised September 29, 2011. Accepted October 15, 2011. Advance Access publication December 20, 2011

Keywords: Charcot–Marie–Tooth disease; disease progression; CMT rat model; biomarker; translation; lipid metabolism

Abbreviations: CMT = Charcot–Marie–Tooth disease; CTSA = cathepsin A; GSTT2 = glutathione S-transferase theta 2; Lpl = lipoprotein lipase; PMP22 = peripheral myelin protein 22; PPARG = peroxisome proliferation-activated receptor gamma

Introduction

Charcot–Marie–Tooth disease (CMT) is the most common inherited neuropathy with a prevalence of up to 1 in 2500 (Skre, 1974; Martyn and Hughes, 1997). In >50% of all cases, the genetic defect underlying CMT is an intrachromosomal duplication spanning 1.4 Mb on human chromosome 17p12, the locus defining CMT subtype 1A (Lupski *et al.*, 1991; Raeymaekers *et al.*, 1991). The gene encoding the peripheral myelin protein of 22 kDa (*PMP22*) is located in the duplicated region and was identified as the responsible disease gene (Matsunami *et al.*, 1992; Patel *et al.*, 1992; Timmerman *et al.*, 1992; Valentijn *et al.*, 1992). Patients with CMT subtype 1A display slowly progressive weakness and atrophy predominantly in distal muscles and absent reflexes with a typical onset at adolescence (Thomas *et al.*, 1997; Krajewski *et al.*, 2000; Shy *et al.*, 2005*b*; Parman, 2007; Pareyson *et al.*, 2009). Patients also show sensory loss and foot deformities. The ultimate clinical phenotype of CMT subtype 1A is determined by the amount of secondary axonal loss (Berciano *et al.*, 2000). Despite its monogenetic cause, patients with CMT subtype 1A display a marked interindividual variability of disease severity, even in the same family and among monozygotic twins (Kaku *et al.*, 1993; Garcia *et al.*, 1995). The reason for this variability is largely unknown and epigenetic factors have been discussed (Steiner *et al.*, 2008; Pareyson *et al.*, 2009).

To date, only physical and electrophysiological examinations are available to determine disease severity in patients with CMT subtype 1A. The CMT neuropathy score is a validated nine-item composite scale taking into account sensory and motor symptoms (Shy *et al.*, 2005*a*). The CMT neuropathy score is currently being applied as the primary outcome measure for CMT subtype 1A trials (Reilly *et al.*, 2010). Neither trials of exercise and orthosis, nor pharmacological approaches with ganglioside, creatine and very recently, oral administration of ascorbic acid showed beneficial effects in patients with CMT subtype 1A (Young *et al.*, 2008; Burns *et al.*, 2009; Micallef *et al.*, 2009; Verhamme *et al.*, 2009; Pareyson *et al.*, 2011). For ascorbic acid, it was suggested that a small effect may have been missed because of unexpectedly slow progression of the disease by only 0.5 CMT neuropathy score points over 2 years (0.25 points per year) (Pareyson *et al.*, 2011) although the progression of the CMT neuropathy score was initially reported to increase ~0.68 points per year (Shy *et al.*, 2005*a*). Thus, limitations of the CMT neuropathy score may underlie the negative therapy outcomes in recent clinical trials (de Visser and Verhamme, 2011; Pareyson *et al.*, 2011).

Surrogate markers of disease severity could add powerful tools to monitor therapeutic effects in clinical trials (Reilly *et al.*, 2010; Pareyson *et al.*, 2011). Furthermore, at present, young patients with CMT subtype 1A cannot be adequately counselled on their individual disease course. Prognostic markers of disease severity would provide patients with important information regarding future life, and also may influence the decision to start a therapy at early time points.

Transgenic rats (CMT rats) that harbour additional copies of *Pmp22* closely phenocopy the pathology and the clinical symptoms of patients with CMT subtype 1A (Sereda *et al.*, 1996, 2003). Importantly, CMT rats kept on an outbred genetic background also develop a highly variable severity of disease, similar to patients with CMT subtype 1A (Sereda *et al.*, 2003). *PMP22* expression measured in skin biopsies from patients with CMT subtype 1A did not correlate with disease severity (Katona *et al.*, 2009) consistent with our data from CMT rats (Meyer zu Hörste *et al.*, 2007). Thus, the need for biomarkers is left open. We therefore addressed the question whether the expression of other genes can be utilized to detect disease severity in CMT subtype 1A. We first examined transcriptional biomarkers for the assessment and prognosis of disease severity in the CMT rat model. We then validated these biomarkers from the CMT rat in skin biopsies of human patients with CMT subtype 1A.

Materials and methods

Transgenic rats

The generation of *Pmp22* transgenic CMT rats has been described previously (Sereda *et al.*, 1996). Routine genotyping was performed by polymerase chain reaction, using genomic DNA from tail biopsies and mouse transgene-specific primers under standard conditions as described (Sereda *et al.*, 1996). All experiments were performed according to the German regulations of Lower Saxony for animal experimentation. Only male rats were used.

Phenotyping

All phenotype analyses were performed by the same investigator who was blinded towards genotype. Motor performance was assessed in standardized grip strength tests for fore-limbs as previously described (Meyer *et al.*, 1979). With their fore-limbs, the animals gripped a horizontal T-bar (width 14 cm, diameter 3.2 mm) connected to a gauge while the investigator pulled their tail proximally from the bar with increasing force. The maximum force (measured in Newton) exerted onto the T-bar before the animals lost grip was recorded.

Hot plate test

This nociceptive test was applied according to a published protocol (Bannon and Malmberg, 2007). Rats were allowed to habituate for 10 min before testing. Pain reflexes in response to a thermal stimulus were measured using a Hot Plate Analgesia Meter (Columbus). The surface of the hot plate was heated to a constant temperature of 55°C, as measured by a built-in digital thermometer with an accuracy of 0.1°C and verified by a surface thermometer. Rats were placed on the hot plate (25.4 × 25.4 cm), which is surrounded by a clear acrylic cage (30 cm high, open top), and the Start/Stop button on the timer

was activated. The latency to respond with either a hindpaw lick, hindpaw flick or jump (which ever comes first) was measured to the nearest 0.1 s by deactivating the timer when the response was observed. The rat was immediately removed from the hot plate and returned to its home cage. If a rat did not respond within 60 s, the test was terminated and the rat removed from the hot plate. Animals were tested one at a time and were not habituated to the apparatus prior to testing. Each animal was tested only once.

Electrophysiological recordings

Nerve conduction velocities and compound muscle action potentials were determined at 9 weeks of age as described previously (Meyer zu Hörste *et al.*, 2007). Briefly, animals were anaesthetized using an intraperitoneal injection of ketamin (100 mg/kg) and xylazin (5 mg/kg), while constant body temperature was maintained using a heating plate connected to a rectal temperature sensor (CMA). Tail nerve conduction velocity proved to be more reproducible than recordings from the sciatic nerve, which had to be exposed surgically. Stimulation was performed with increasing voltage until supramaximal stimulation was achieved. Maximum compound muscle action potential voltage was recorded from tail muscle with fine subcutaneous needle electrodes using a Jaeger–Toennies Neuroscreen instrument. Compound muscle action potential amplitudes were calculated peak to peak. Nerve conduction velocity was calculated from distance and motor latency differences between proximal and distal stimulations.

Tissue preparation

At post-natal Day 5, a skin biopsy from the tail was collected from each animal after short CO_2 narcosis, for genotype determination by polymerase chain reaction. Sciatic nerve and skin biopsies (from operation wound) were taken at post-natal Day 7, before onset of disease, and collected in liquid nitrogen and stored at −80°C. After 9 weeks of age (Day 63), all rats were sacrificed by CO_2 narcosis. Again, one skin biopsy from the tail was dissected from each animal, collected on liquid nitrogen and stored at −80°C. At both time points, Days 7 and 63, the surrounding connective and fatty tissue of the sciatic nerve, found in the epineurium, was carefully removed with a razor blade. Then the animal was perfused with Hanks' buffered salt solution, followed by a modified fixation with 2.5% glutaraldehyde and 4% paraformaldehyde in phosphate buffer (Karlsson and Schultz, 1965; Sereda *et al.*, 1996).

Histology of peripheral nerve

After perfusion, one tibial nerve was dissected and embedded in epoxy resin (Luft, 1961). Semi-thin sections (0.5 µm) of tibial nerves were cut at level with the medial ankle. Sections were stained with methylene blue-Azur II and photographed using a standard video frame grabber (ProgRes C14, Jenoptic) installed on a Zeiss Axiophot microscope. Overlapping photographs of the entire nerves were taken and merged using PanoToolsAssembler software. After blinding, the entire number of axons per tibial nerve was counted manually by the same investigator using the CellCounter plugin of ImageJ (v1.36, NIH). Each individual axon was manually marked and automatically counted. Physiologically unmyelinated axons (diameter <1 µm) and Remak-bundle fibres were not included.

RNA isolation, labelling and microarray hybridization

RNA preparation was performed according to the manufacturer instructions without adding any carrier (RNeasy® Lipid tissue Mini Kit, Qiagen). RNA quality and quantity of control samples was checked by analysing aliquots on the Agilent 2100 Bioanalyser using the RNA 6000 Pico LabChip kit (Agilent Technologies). Total RNAs of all sample groups were stored at −80°C and were processed in parallel. Immediately before amplification, RNA was precipitated by adding Na-acetate (pH 5.2, 0.3 M, final concentration), 2 µl of PelletPaint (Calbiochem; Novabiochem) and ethanol. Total RNA was resuspended with pretested T7-tagged dT21V oligonucleotides as previously described (Rossner *et al.*, 2006). One-round T7-RNA polymerase-mediated linear amplification and biotin labelling was performed according to specifications given by the manufacturer (Affymetrix). Biotin-labelled amplified RNA size distribution and quantity was analysed with the Agilent 2100 Bioanalyser using the RNA 6000 Nano LabChip kit (Agilent Technologies). Hybridization, washing, staining and scanning were performed under standard conditions as described by the manufacturer (Affymetrix). Rat Gene 1.0 ST tiling arrays were used that cover more than 27 000 transcripts.

Microarray data analysis

Data analysis was performed using the integrated software packages Genomics Suite (Partek Inc.) and R-scripts (www.bioconductor.org). Raw data were normalized using the RMA algorithm and differentially expressed genes were identified with ANOVA according to the workflow suggested by the manufacturer and with cut-offs at >1.3-fold change and *P*-values <0.001 (Partek Inc.). The identification of coordinated changes in *a priori* defined sets of functionally grouped genes was performed using the Gene Set Enrichment Analysis approach (Mootha *et al.*, 2003). The gene set enrichment analysis software package was downloaded and locally implemented (www.broadinstitute.org/gsea) and used with default parameters (permutations set to 1000) and all available gene sets available in the molecular signature database (MSigDB v3.0).

Semi-quantitative real time-polymerase chain reaction

Real time-polymerase chain reaction reactions (SYBR® Green polymerase chain reaction assay for rat tissue, TaqMan® polymerase chain reaction assay for human tissue) were carried out using the ABI Prism 7500 Sequence Detection System (Applied Biosystems). A real time-polymerase chain reaction master mix was prepared to a final reaction volume of 10 µl. The real time-polymerase chain reaction followed the standard two-step protocol and quantitation of polymerase chain reaction product was performed using the comparative ΔΔCt method as recommended by the manufacturer. All real time-polymerase chain reactions were carried out in triplicate and averaged. All TaqMan® primers and probe sets were designed using the primer express software V.1.65 (Applied Biosystems). For quantification of expression levels total complementary DNA amplification was normalized against the most stable pair of housekeeping genes calculated by GeNorm Software (Vandesompele *et al.*, 2002) (messenger RNAs of actin beta and cyclophilin A for rat tissue and actin beta and microtubulin beta 2 for human tissue). Real time-polymerase chain reaction was carried out for weakly, intermediate and severely affected CMT rats and wild-type rats on an individual level. The lowest gene of

interest expression was defined as 1.0-fold relative expression for all samples/groups. The sequences of polymerase chain reaction primers and fluorescent probe sequences (TaqMan®) can be provided upon request.

Patient evaluation and Charcot–Marie–Tooth neuropathy score

Forty-six patients with CMT subtype 1A were prospectively evaluated at the Friedrich Baur Institut at the University of Munich ($n = 25$) and at the Department of Clinical Neurophysiology at the University of Göttingen ($n = 21$) by two examiners (B.S.W. and M.W.S.). Evaluation consisted of a detailed history, a neurological examination and electrophysiological studies. Primary clinical outcome was the CMT neuropathy score, as indicated by the 136th European Neuro Muscular Centre workshop (Reilly *et al.*, 2006). The CMT neuropathy score is a validated nine-item (36 point) composite scale taking into account sensory and motor symptoms and signs in upper and lower limbs, and amplitudes of M-response and of sensory action potential of the ulnar nerve (Shy *et al.*, 2005*a*). In addition, secondary clinical parameters comprised: (i) maximal voluntary isometric contraction as determined with a myometer, for distal arm (hand grip, three-point pinch) and leg (foot flexion/extension) movements; (ii) Overall Neuropathy Limitations Scale; (iii) Timed 10-m Walk Test; (iv) Nine-hole-peg Test; (v) Visual Analogue Scale for pain and fatigue and (vi) health-related quality of life (36 item Short Form questionnaire) (Ware and Sherburne, 1992).

Skin biopsies

The skin biopsy of the patient was taken from the proximal, medial part of the index finger of the non-dominant hand at the end of all examinations to avoid any influences of other test results. The surgery was performed under sterile conditions of the operation field as well as under local anaesthesia with 1% lidocaine. The sterile disposables of 3 mm, biopsy punch by Stiefel was used and sterile steri-strips (3M) were applied. The skin biopsy was separated into two equal parts, one placed in 4% paraformaldehyde in 1× phosphate-buffered saline, the other in RNAlater® (Ambion). To avoid any damage, the biopsies were carried in a box with ice to the laboratory and stored at −20°C (RNAlater®) and 4°C (paraformaldehyde) for further examination.

Statistical analysis

All values are expressed as mean ± SEM unless indicated otherwise. All data were tested on Gaussian distribution (Kolmogorow–Smirnow–Lilliefors test) and where applicable, used parametric (Student's *t*-test) or non-parametric (Willcoxon–Mann–Whitney U-test) testing. Correlation analyses were performed using the Spearman's rank correlation test. Statistica 6.0 (StatSoft) was used for statistical analyses in rats.

Statistical analysis of human real time-polymerase chain reaction expression analysis with regard to collected clinical data was performed by U.H. and W.K. and is extensively described in a statistical report in Supplementary material. Analysis was performed via step-wise linear regression with forward and backward stepping procedures. The variables in the multiple linear model for CMT neuropathy score were used to determine multiplicity adjusted *P*-values and were presented in addition to the usual *P*-values to assess the statistical association of markers and demographic variables with CMT neuropathy score. Leverage plots were used to visualize the association of the individual data of each variable with the target variable in the multiple linear models.

Results

Charcot–Marie–Tooth rats display clinical variability

In 50 randomly chosen CMT rats, skin and sciatic nerve samples were collected both at Day 7, i.e. before onset of clinical phenotype, and again at 9 weeks of age (Day 63) when they display clinical impairments (Fig. 1A).

The progression of the clinical phenotype was tracked by grip strength measurements at 3, 5, 7 and 9 weeks of age, demonstrating significant differences between wild-type rats ($n = 6$) and CMT rats ($n = 50$) from 5 weeks onwards ($P < 0.05$; Fig. 1B). The grip strength at 9 weeks of age, when rats were sacrificed, was used for the identification of mildly and severely affected CMT rats (Fig. 1B). In order to strengthen the primary selection criterion, rats with most extreme values in grip strength were also subjected to electrophysiological (Fig. 1C and D), nociceptive (hot plate) (Fig. 1G and H) and histological (Fig. 1E and F) analysis.

Electrophysiological recordings (representative traces in Fig. 1C) revealed a reduction in compound muscle action potential amplitudes in CMT rats compared with wild-type rats (4.91 ± 0.59 mV; $n = 9$). Importantly, severely affected CMT rats (1.32 ± 0.16 mV; $n = 10$) showed a further decrease in compound muscle action potentials compared with mildly affected rats (3.25 ± 0.37 mV; $n = 7$) (Fig. 1D). In contrast, nerve conduction velocities were significantly lower in CMT rats compared with wild-type rats whereas no difference was observed between mildly and severely affected CMT rats (data not shown). This suggests that the extent of axonal loss rather than demyelination determines individual differences of disease severity (Meyer zu Hörste *et al.*, 2007).

Additionally, we analysed the sensory phenotype of CMT rats with the nociceptive hot plate test where rats respond to heat pain by hindpaw licking (Fig. 1G). Pain response latencies were unaltered between wild-type animals (28.98 ± 2.95 s) and mildly affected CMT rats (33.95 ± 2.06 s) but we observed a significant sensory impairment in severely affected CMT rats (46.63 ± 2.62 s, $P < 0.005$ compared with wild-type and mildly affected CMT rats). That nociceptive impairments correlate with disease severity, whereas motor nerve conduction velocity does not, may best be explained by sensory axon loss.

The histological analysis of tibial nerve cross sections revealed hypomyelinated axons next to axonal loss and increased abundance of connective tissue in CMT rats (Fig. 1E; see also Sereda *et al.*, 1996). These common features of CMT subtype 1A pathology were most prominent in severely affected CMT rats (Fig. 1E). The absolute number of myelinated axons per tibial nerve, as a direct measure of disease severity, was significantly different between wild-type rats (2963 ± 33 axons; $n = 4$), mildly affected CMT rats (2811 ± 23 axons; $n = 7$) and severely affected CMT rats (2672 ± 19 axons; $n = 10$) (Fig. 1F).

To reliably identify differentially affected CMT rats, two robust phenotype measures, grip strength and the absolute number of

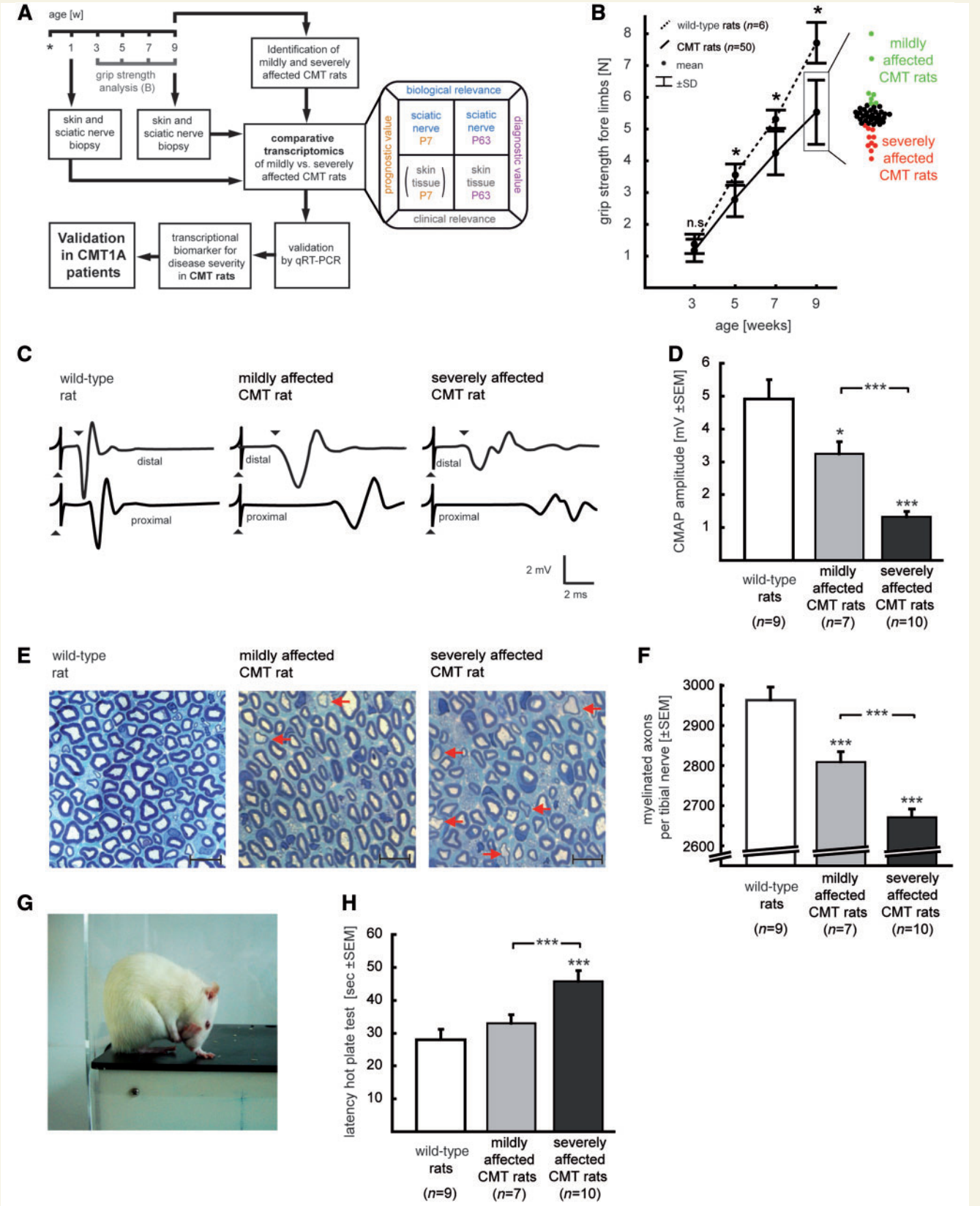

Figure 1 CMT rats show high clinical variability. (**A**) At post-natal Day 7 (P7), biopsies of sciatic nerve and skin tissue were taken. Phenotype analysis was then performed at the age of 3, 5, 7 and 9 weeks by measuring the grip strength of the fore-limbs. At 9 weeks of age, all rodents were sacrificed. Tibial nerve was assessed for histology and again, skin and sciatic nerve tissue were sampled for transcriptional analysis. After identification of severely and mildly affected CMT rats ($n = 5$ each), sciatic nerve (biologically relevant) and skin tissue (clinically relevant) samples were analysed by gene expression profiling to identify putative prognostic (Day 7) and disease severity

(continued)

myelinated axons per tibial nerve were combined and a CMT rat neuropathy score was generated (Table 1 and Supplementary Fig. 1). Next, five CMT rats with the highest and the lowest CMT rat neuropathy score each were selected for comparative transcriptome analysis, and are henceforward referred to as mildly affected CMT rats (CMT rat neuropathy score 0–3) and severely affected CMT rats (CMT rat neuropathy score 9–10). All remaining rats were grouped as moderately affected animals (CMT rat neuropathy score 4–8).

RNA expression profiles in sciatic nerve codefine the clinical severity in Charcot–Marie–Tooth rats

Comparative microarray analysis was performed with messenger RNA samples derived from Day 7 and Day 63 sciatic nerve of mildly affected and severely affected CMT rats applying three biological replicates in each group. We identified dysregulated genes via the criteria magnitude of regulation (1.5-fold) and level of significance ($P < 0.05$). In sciatic nerve, at Day 7, 74 genes were upregulated and five genes downregulated and at Day 63, 81 genes were upregulated and 132 genes downregulated in severely affected compared with mildly affected CMT rats (Table 2). By annotation of dysregulated messenger RNAs using gene ontology, a pronounced involvement of metabolic processes with regard to disease severity was detected in sciatic nerve tissue (Fig. 2A). The proportion of metabolism related dysregulated genes was more prominent at Day 63 compared with Day 7. To further specify the dysregulated genes, we used a knowledge-based approach; the gene set enrichment analysis (Subramanian *et al.*, 2005). Importantly, we identified a strong dysregulation of genes involved in the metabolism of lipids (Fig. 2B). Most lipid metabolism associated genes were downregulated in sciatic nerves of CMT rats when compared with wild-type animals in development (Day 7) as well as in young adulthood (Day 63) (Fig. 2B). At Day 7, lipid metabolism associated genes showed an average upregulation in severely affected compared with mildly affected CMT rats, whereas an inverse regulation was observed at the age of 9 weeks (Day 63) (Fig. 2B).

Validation of candidate genes via real time-polymerase chain reaction in sciatic nerve

For validation by real time-polymerase chain reaction at the single animal level ($n = 5$ per group), we selected the most prominent dysregulated candidate messenger RNAs of different gene sets (Table 3). In particular, genes involved in fatty acid metabolism and cell growth were found to be predominantly dysregulated at both time points (11 genes at Day 63, six genes at Day 7).

Table 1 Identification of mildly and severely affected CMT rats by applying a CMT rat neuropathy score

CMT rat neuropathy subscore	0	1	2	3	4	5
Axons per tibial nerve	>2850	>2800	>2750	>2700	>2650	⩽2650
Grip strength fore-limbs	>6.5	>6	>5.5	>5	>4.5	⩽4.5
CMT rat neuropathy score = axons per tibial nerve + grip strength fore-limbs (max 10)						
CMT rat neuropathy score 0–3:	Mildly affected					
CMT rat neuropathy score 4–8:	Moderately affected					
CMT rat neuropathy score 9–10:	Severely affected					

Myelinated axons per tibial nerve and fore-limb grip strength define the CMT rat neuropathy score. For each parameter, six score classes were designed with respect to decrease in axon number and grip strength. The CMT rat neuropathy score was composed by adding both parameter scores (myelinated axons per tibial nerve and fore-limb grip strength) resulting in a maximum CMT rat neuropathy score of 10. Three disease severity classes were then specified: mildly affected, CMT rat neuropathy score 0–3; moderately affected, CMT rat neuropathy score 4–8; and severely affected, CMT rat neuropathy score 9–10.

Figure 1 Continued
(Day 63) markers. (**B**) Grip strength analysis (fore-limbs) of wild-type (dotted line) in comparison with CMT rats (continuous line) at 3, 5, 7 and 9 weeks of age (mean, SD, $*P < 0.05$, Student's *t*-test). Individual grip strength values are depicted on the right, defining mildly ($n = 7$) and severely ($n = 10$) affected CMT rats at 9 weeks of age (green and red dots, respectively). These animals were then chosen for electrophysiological (**C** and **D**), histological (**E** and **F**) and nociceptive hot plate analysis (**G** and **H**) and compared with wild-type controls ($n = 10$). (**D**) Quantification of compound muscle action potentials (CMAP) recorded after proximal stimulation show a significant decrease from wild-type rats to mildly and severely CMT rats. Representative traces for each group are depicted in (**C**) (▲ = stimulus, ▼ = distal motor latency). (**E**) Representative light microscopic pictures of tibial nerve cross sections of wild-type rats and mildly- and severely affected CMT rats, aged 9 weeks. Arrows depict demyelinated axons, which are increased in severely, compared with mildly affected animals (scale bar = 10 μm). (**F**) Quantification of total myelinated axons per tibial nerve in 9-week-old rats. A significant decrease in axon number was observed when comparing wild-type rats to mildly and severely affected CMT rats. (**G**) Nociceptive hot plate analysis was performed by placing rats on a 55°C thermo plate and measuring latency to pain response as defined by hindpaw licking. (**H**) Latencies increased when comparing mildly to severely affected CMT rats, but not between comparing wild-type and mildly affected. Asterisks upon boxes indicate significant differences to age and sex matched wild-type control animals. (mean; SEM; $*P < 0.05$, $***P < 0.005$). qRT-PCR = semi-quantitative real time-polymerase chain reaction.

Table 2 Microarray analysis of severely compared with mildly affected CMT rats

Tissue/time point	Upregulated in severely versus mildly affected CMT rats	Downregulated in severely versus mildly affected CMT rats
Sciatic nerve Day 7	74	5
Sciatic nerve Day 63	81	132
Skin Day 63	203	142

At Day 7, 74 genes were upregulated and five genes downregulated in sciatic nerves of CMT rats, which are severely affected at Day 63 when compared with mildly affected CMT rats. At Day 63, 81 genes were upregulated and 132 genes downregulated in severely versus mildly affected CMT rats. In skin biopsies of Day 63 CMT rats, 203 genes were upregulated and 142 downregulated in severely affected CMT rats when compared with mildly affected. Criteria for selection was a fold change of >1.5 and a *P*-value <0.05.

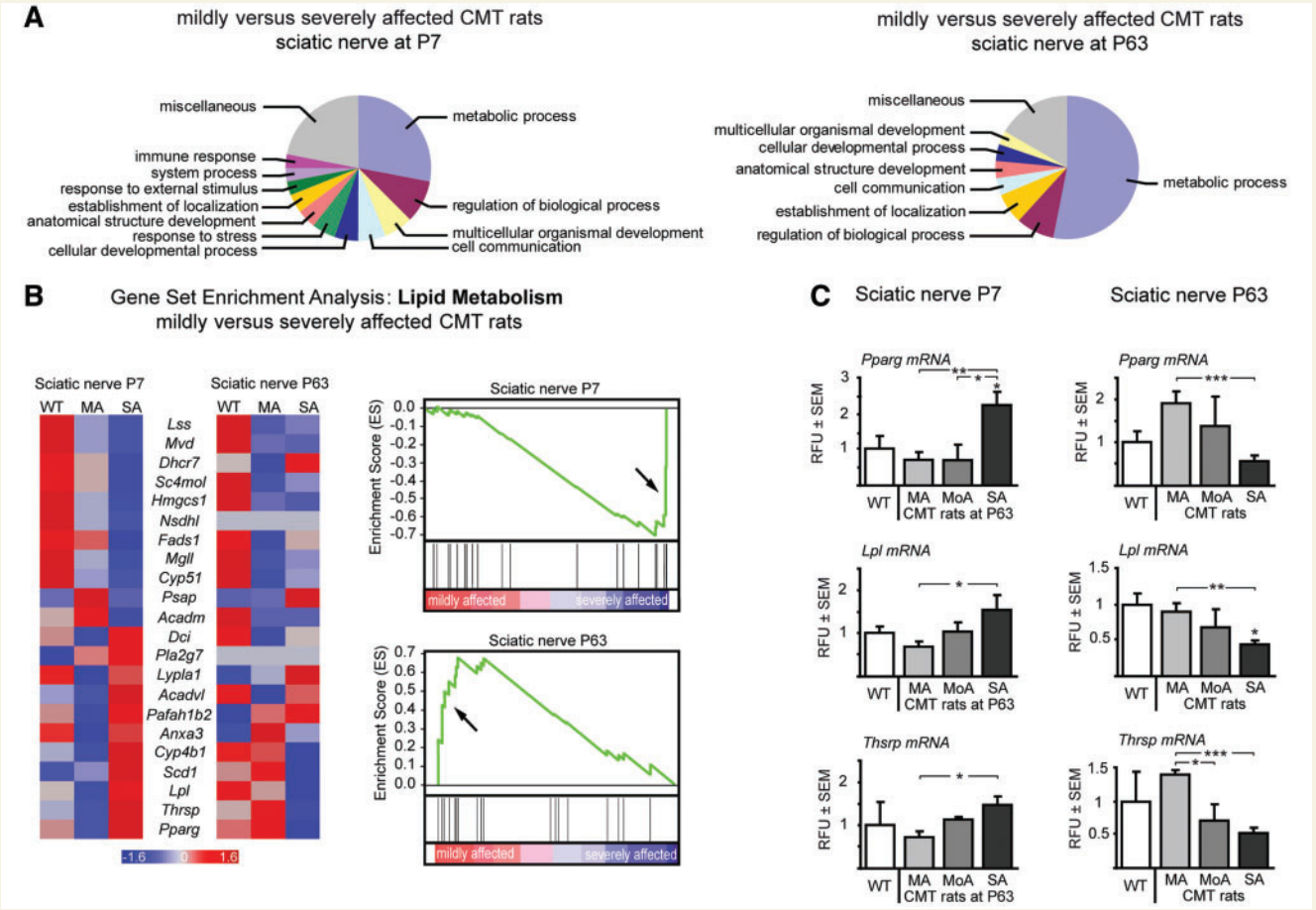

Figure 2 Dysregulated lipid metabolism in sciatic nerve of CMT rats codefines clinical severity. (**A**) Pie charts of dysregulated genes in sciatic nerves between mildly and severely affected CMT rats with the annotation to gene ontology classes at Day 7 (P7, *left*) and Day 63 (P63, *right*). Genes associated with metabolic processes increase with age. (**B**) Gene set enrichment analysis (GSEA) revealed pronounced downregulation of genes involved in lipid metabolism in sciatic nerve from mildly (MA) and severely affected (SA) CMT rats compared with wild-type rats (WT) at Day 7 and Day 63. Heatmap plots (*left*) show dysregulation of lipid metabolism related genes with respect to disease severity. The direction of regulation for the lipid metabolism gene set is inversed at Day 7 compared with Day 63, visualized in enrichment plots (*right*, indicated by arrows). (**C**) Validation of selected candidate messenger RNAs *Pparg*, *Lpl* and *Thrsp* was performed by semi-quantitative real time-polymerase chain reaction. Expression of wild-type rats, mildly affected (MA, as defined by a CMT rat neuropathy score of 0–3), moderately affected (MoA, CMT rat neuropathy score 4–8) and severely affected CMT rats (SA, CMT rat neuropathy score 9–10) are shown ($n = 5$ each). At Day 63, severely affected CMT rats show downregulation of depicted genes compared with mildly affected CMT rats. However, at Day 7, selected genes are upregulated in animals which display a severe phenotype at Day 63. Asterisk upon bar indicates significant difference to wild-type expression level (RFU = relative fluorescent units; mean; SEM; *t*-test $^*P < 0.05$, $^{**}P < 0.01$, $^{***}P < 0.005$).

Table 3 Validated prognostic and disease severity markers in CMT rats

		Prognostic markes				Disease severity markers			
		Sciatic nerve (Day 7)		Skin (Day 7)		Sciatic nerve (Day 63)		Skin (Day 63)	
Function	Gene	Ratio	*P*-value	Ratio	*P*-value	Ratio	*P*-value	Ratio	*P*-value
Fatty acid metabolism	*Adipoq*	3.07	0.030	1.27	0.459	0.34	0.024	3.96	0.108
	Lpl	2.20	0.050	2.09	0.690	0.49	0.009	3.20	0.105
	Scd1	1.85	0.074	0.58	0.549	0.52	0.591	1.73	0.150
	Pparg	3.17	0.009	1.69	0.170	0.26	0.004	3.17	0.045
	Prkar2b	1.28	0.529	0.83	0.115	0.57	0.044	2.70	0.054
	Ssg1	1.75	0.078	1.23	0.338	0.48	0.007	2.97	0.015
	Thrsp	2.05	0.029	0.76	0.567	0.23	0.000	2.96	0.067
Metabolism	*Cdo1*	2.02	0.087	1.09	0.765	0.32	0.011	6.25	0.221
	Gstp2	1.14	0.371	1.33	0.083	1.07	0.446	1.27	0.086
	Gstt2	0.88	0.336	1.39	0.039	1.16	0.306	1.44	0.005
	Car3	2.74	0.028	0.70	0.539	0.29	0.027	3.16	0.047
	Nnt	0.82	0.504	1.24	0.349	1.00	0.982	1.82	0.034
	Ctsa	0.96	0.768	1.48	0.044	1.00	0.998	2.23	0.000
Growth factor	*Gdnf*	2.03	0.071	2.16	0.276	0.64	0.019	1.35	0.380
	Igf1	1.07	0.779	1 02	0.996	0.37	0.003	4.41	0.046
	Igfbp5	1.89	0.039	1.07	0.660	0.78	0.208	3.34	0.012
	Rbp4	2.66	0.073	1.16	0.492	0.54	0.014	2.77	0.098
	Tgfb3	1.34	0.224	1.99	0.022	0.72	0.067	1.78	0.089
Cytoskeleton	*Dpt*	1.62	0.291	1.42	0.126	0.71	0.216	1.86	0.034
	Myl1v2	5.31	0.359	1.71	0.374	0.85	0.742	7.65	0.081
	Sprr1al	1.16	0.583	0.62	0.233	1.42	0.052	0.34	0.014
	Nefl	2.68	0.012	1.30	0.808	1.11	0.871	1.22	0.511
	Nefm	2.44	0.035	n.d.	n.d.	1.05	0.921	4.37	0.134
	Nexn	1.78	0.079	1.68	0.213	1.36	0.026	1.84	0.115
Inflammation	*Cxcl12*	1.33	0.239	1.57	0.026	0.83	0.320	1.68	0.058
	Ddt	1.05	0.801	0.52	0.383	1.12	0.452	1.29	0.010
	Ebf1	1.49	0.070	1.06	0.842	0.90	0.301	2.26	0.065
	Il16	1.03	0.890	1.02	0.974	1.28	1.181	1.62	0.011
	Il1r1	1.42	0.061	1.38	0.266	1.06	0.371	1.27	0.056
Myelin	*Cldn1*	1.95	0.035	1.70	0.141	1.03	0.935	1.20	0.260
	Pmp22	1.39	0.345	1.82	0.037	1.33	0.067	1.48	0.272
	Prx	1.25	0.092	1.53	0.343	1.32	0.023	1.95	0.054
Intracellular signalling	*Pde2a*	1.83	0.164	1.16	0.635	1.01	0.950	2.17	0.056
	Pde3b	1.22	0.499	1.10	0.696	0.67	0.102	3.06	0.086
	Fn3krp	0.91	0.072	0.73	0.599	1.14	0.008	1.54	0.018
Transcription factors	*Id3*	1.77	0.102	1.44	0.016	0.86	0.143	1.60	0.067
	Ribin	1.36	0.097	0.95	0.637	1.16	0.216	0.84	0.010

$P < 0.05$	$P < 0.1$	$P < 0.1$	$P < 0.05$
upregulated in severely affected CMT rats		downregulated in severely affected CMT rats	

Putative disease severity and prognostic biomarker candidates were identified by comparative microarray analysis of Day 63 skin and sciatic nerve and Day 7 sciatic nerve messenger RNA (Figs 2 and 3; Table 2). Depicted are differentially expressed genes validated by semi-quantitative real time-polymerase chain reaction at the single animal level ($n = 5$) in both sciatic nerve and skin at Day 7 and Day 63. Validated genes were annotated to known functions. The ratio of mean expression values of severely and mildly affected CMT rats is indicated with *P*-value (ratio >1: upregulation in severely affected CMT rats). Upregulated genes in severely affected CMT rats are highlighted in red, whereas downregulated genes are highlighted in blue (dark: $P < 0.05$; light: $P < 0.01$, respectively). *Adipoq* = adiponectin; *Car3* = carbonic anhydrase 3; *Cldn1* = claudin 1; *Ctsa* = cathepsin A; *Cxcl12* = chemokine ligand 12 C-X-C motif; *Ddt* = dopachrome D-tautomerase; *Dpt* = dermatopontin; *Ebf1* = early B-cell factor 1; *Fn3krp* = rouctosamine 3 kinase related protein; *Gdnf* = glial cell line derived neurotrophic factor; *Gstp2* = glutathione S-transferase, pi, type 2; *Gstt2* = glutathione S-transferase, theta, type 2; *Id3* = inhibitor of DNA binding 3; *Igf1* = insulin-like growth factor 1; *Igfbp5* = insulin-like growth factor binding protein 5; *Il16* = interleukin 16; *Il1r1* = interleukin 1 receptor 1; *Myl1v2* = myosin light chain 1, variant 2; *Nefl* = neurofilament light chain; *Nefm*; neurofilament medium chain; *Nexn* = nexilin; *Nnt* = nicotinamide nucleotide transhydrogenase; *Pde2a* = phosphodiesterase 2b; *Pde3b* = phosphodiesterase 3b; *Pmp22* = peripheral myelin protein 22 kDa; *Prkar2b* = protein kinase, cAMP-dependent, regulatory, type II, beta; *Prx* = periaxin; *Rbp4* = retinol binding protein 4; *Ribin* = rRNA promoter binding protein; *Scd1* = stearoyl Co-A-desaturase1; *Sprr1al* = small proline rich repeat protein 1a like; *Ssg1* = steroid sensitive gene 1; *Tgfb3* = transforming growth factor, beta 3; *Thrsp* = thyroid hormone responsive; *Cdo1* = cysteine dioxygenase 1.

Next, we validated the three most strongly regulated genes of the lipid metabolism gene set (identified by gene set enrichment analysis; Fig. 2B) via real time-polymerase chain reaction and extended our analysis to moderately affected CMT rats and wild-type animals (Fig. 2C). In the Day 63 sciatic nerve, the messenger RNA expression ratios for the *Pparg*, lipoprotein lipase (*Lpl*) and thyroid hormone responsive protein (*Thrsp*) genes in sciatic nerve were decreased in severely affected compared with mildly affected CMT rats (fold changes: peroxisome proliferation-activated receptor gamma (*Pparg*) = 0.26, $P < 0.005$; *Lpl* = 0.49, $P < 0.01$; *Thrsp* = 0.23, $P < 0.001$; Fig. 2C and Table 3). Conversely, in the Day 7 sciatic nerve, the relative messenger RNA expression levels of these genes were increased in CMT rats with severe disease progression compared with CMT rats with a mild disease progression (fold changes: *Pparg* = 3.17, $P < 0.01$; *Lpl* = 2.20, $P < 0.05$; *Thrsp* = 2.05, $P < 0.05$; Fig. 2C and Table 3). In summary, messenger RNA levels of lipid metabolism associated genes correlated with disease variability in sciatic nerve of CMT rats displaying an inverted expression when comparing early and late disease stages.

Prognostic and disease severity markers validated in skin biopsies of Charcot–Marie–Tooth rats

In the skin of CMT rats, hypomyelinated fibres can be observed in subcutaneous nerve bundles, which share features with the pathology of the sciatic nerve (Fig. 3A). Comparative gene expression profiling of mildly affected versus severely affected CMT rats (Day 63) using skin tissue derived messenger RNA was performed with two technical replicates of five pooled samples per group. This approach resulted in 203 upregulated and 142 downregulated genes with respect to the criteria fold change (1.5) and significance ($P < 0.05$) (Table 2). Gene ontology annotation of dysregulated genes identified messenger RNAs related to cellular processes, to development/growth and, like in sciatic nerve tissue, to metabolic processes (Fig. 3B and Table 3). Microarray analysis of skin tissue biopsied at Day 7 was not performed due to the low amount of isolated RNA.

Validation of biomarker candidates via real time-polymerase chain reaction in skin biopsies of Charcot–Marie–Tooth rats

At Day 63, most transcripts validated via real time-polymerase chain reaction (14 genes, $P < 0.05$; Table 3) showed an upregulation in the skin of severely affected when compared with mildly affected CMT rats. Six genes were also differentially regulated at Day 7 as shown by real time-polymerase chain reaction ($P < 0.05$; Table 3).

We then selected several candidates for extended real time-polymerase chain reaction validation in skin including moderately affected CMT rats and wild-type controls (in addition to severely and mildly affected CMT rats). Among the validated transcripts, glutathione S-transferase theta 2 (*Gstt2*) and cathepsin A (*Ctsa*) were found to be co-regulated in skin at both time points when comparing severely and mildly affected CMT rats (Table 3). The relative expression ratios of the selected cutaneous disease severity markers in severely affected versus mildly affected CMT rats at Day 7 were 1.44 ($P < 0.05$) for *Gstt2* and 1.48 ($P < 0.05$) for *Ctsa* (Fig. 3C and Table 3). At Day 63, the correlation with disease severity was even stronger, with a 1.44-fold change ($P < 0.01$) for *Gstt2* and 2.23 ($P < 0.001$) for *Ctsa* (Fig. 3C and Table 3). Importantly, *Gstt2* messenger RNA was also validated as a surrogate marker for disease severity in skin tissue after a successful therapeutic approach in CMT rats, which we had performed previously (Supplementary Fig. 2; see also Meyer zu Hörste *et al.*, 2007).

Pparg was validated as a marker for disease severity in skin at Day 63 (3.17-fold change, $P < 0.05$; Fig. 3C). However, *Pparg* was not identified as a prognostic marker in skin, but in sciatic nerve tissue (Table 3). Finally, *Pmp22* was validated as a prognostic marker in skin at Day 7 (1.82-fold change, $P < 0.05$). Importantly, *Pmp22* was not identified as a disease severity marker in cutaneous and sciatic nerve tissue at Day 63 (Table 3).

Biomarker validation in skin biopsies from patients with Charcot–Marie–Tooth subtype 1A

In order to translate our findings from the CMT rat directly to affected patients, we clinically examined the disease severity of 46 patients with genetically confirmed CMT subtype 1A, applying the CMT neuropathy score in addition to secondary outcome measures (Shy *et al.*, 2005*a*) (Table 4). We analysed 19 male and 27 female patients with CMT subtype 1A, aged 44.6 ± 12.7 years (mean $\pm$ SD), and the average CMT neuropathy score was calculated to be 14.6 ± 5.8 points (mean $\pm$ SD) (Table 4). This average disease severity fits well with reports from other clinical studies (Shy *et al.*, 2008; Pareyson *et al.*, 2011). We next sampled skin biopsies of this CMT subtype 1A cohort to validate putative disease severity markers. We chose five genes as the most promising candidates using the criteria fold change and co-regulation between different time points and tissues in the CMT rat (Table 3).

Exploratory statistical linear regression modelling was used to identify surrogate disease severity markers and variables for the CMT neuropathy score (Fig. 4A). The variables of the resulting models were used in addition to model the CMT neuropathy score subcategories of sensory symptoms (Fig. 4B) and motor symptoms (Fig. 4C) (for complete statistical report see Supplementary material).

Importantly, the marker *GSTT2* messenger RNA significantly influenced all three CMT neuropathy score-related models. The *P*-values for *GSTT2* messenger RNA were found to be $P = 0.0006$ for the CMT neuropathy score, $P = 0.0002$ for sensory symptoms and $P = 0.0126$ for motor symptoms. The marker *CTSA* messenger RNA showed a considerable statistical influence in the CMT neuropathy score-related models, but not to the same degree and with the same consistency as *GSTT2* (CMT neuropathy score, $P = 0.0065$; sensory symptoms, $P = 0.0313$; motor

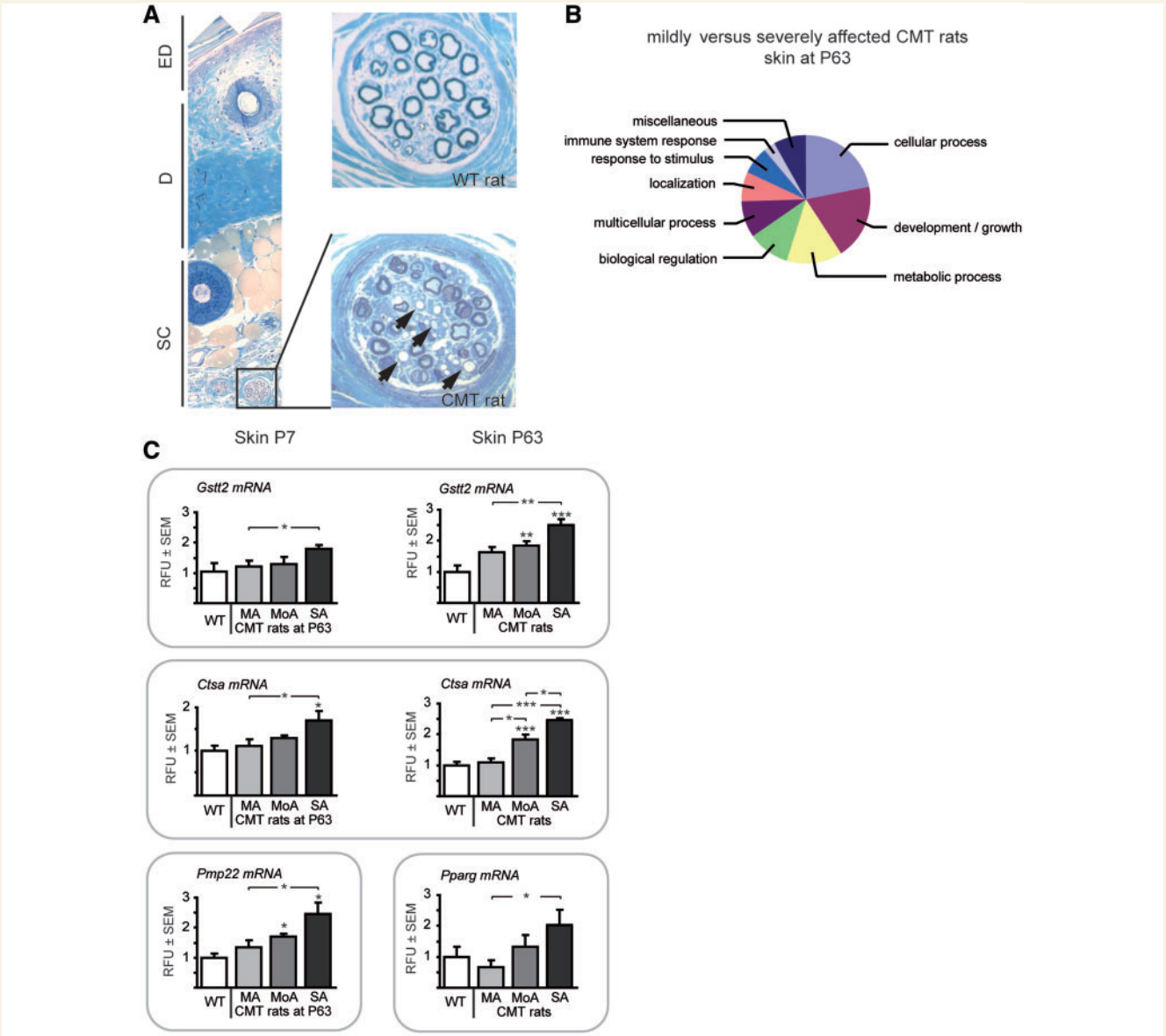

Figure 3 Cutaneous messenger RNA disease severity markers in CMT rats. (**A**) Light microscopic (scale bar = 50 μm) image of methylene blue stained cross section of rat skin. Three dermal layers can be discriminated: epidermis (ED), dermis (D) and subcutis (SC). Subcutaneous nerve fibre bundles can be found and hypomyelination of axons in dermal nerve fibres of CMT rat is evident compared with wild-type (WT) control animal (indicated by arrows, scale bar = 10 μm). (**B**) Pie chart of dysregulated genes in skin between mildly (MA) and severely (SA) affected CMT rats with annotation to gene ontology classes at Day 63. (**C**) Validation of selected candidate messenger RNAs *Gstt2*, *Ctsa*, *Pmp22* and *Pparg* was performed by semi-quantitative real time-polymerase chain reaction. Expression of wild-type rats, mildly affected (MA, CMT rat neuropathy score 0–3), moderately affected (MoA, with a CMT rat neuropathy score, CMT rat neuropathy score of 4–8) and severely affected CMT rats (SA, CMT rat neuropathy score 9–10) are shown ($n = 5$ each). At Day 63 (*right*), severely affected CMT rats show upregulation of *Gstt2*, *Ctsa* and *Pparg* messenger RNA levels compared with mildly affected CMT rats. However, at Day 7 (*left*), messenger RNA levels of *Gstt2*, *Ctsa* and *Pmp22* are upregulated in skin tissue of CMT rats, which display a severe disease phenotype at Day 63 (SA, CMT rat neuropathy score 9–10). Asterisks upon bar indicates significant difference to wild-type expression level (mean, SEM, *t*-test $*P < 0.05$, $**P < 0.01$, $***P < 0.005$). RFU = relative fluorescent units.

symptoms, $P = 0.0114$). As expected, age significantly correlated with the disease variability and was therefore also included in CMT neuropathy score-related surrogate marker models (CMT neuropathy score, $P = 0.0042$; sensory symptoms, $P = 0.0713$; motor symptoms, $P = 0.0032$). In multiple linear regression models, potentially predictive markers/parameters for CMT neuropathy score should have an adjusted *P*-value (see Supplementary material), which has to be below the standard alpha level of 0.05 (Table 4). Importantly, this holds true in the CMT neuropathy score model for the marker *GSTT2* with an adjusted *P*-value of

Table 4 Clinical examinations of 46 patients with CMT subtype 1A

	Mean (SD)	Median (Interquartile range)
Age (years)	44.6 (12.7)	47.0 (16.3)
CMT neuropathy score	14.6 (5.8)	13.0 (8.0)
Compound muscle action potential (mV)	2.2 (1.7)	1.7 (2.6)
Sensory nerve action potential (μV)	4.4 (9.4)	0.4 (5.8)
10-m Walking Test (s)	6.1 (3.3)	5.5 (3.8)
Nine-peg-hole Test (s)	27.3 (18.9)	22.3 (6.5)
VAS-value (mm)	29.4 (29.9)	24.0 (49.0)
Maximal voluntary isometric contraction (*N*)		
Fist grip	88.0 (52.3)	74.8 (63.5)
3-Point grip	52.6 (27.6)	48.8 (29.4)
Pinch grip	31.2 (24.8)	25.3 (23.8)
Foot dorsiflexion	19.7 (21.9)	15.0 (24.2)
Foot plantar flexion	73.3 (59.5)	53.0 (103.7)

In the cohort of 46 probands with an average age of 44 years (mean = 44.6; SD = 12.7) we performed the CMT neuropathy score and secondary outcome measures of disease severity in genetically confirmed patients with CMT subtype 1A. We performed neurophysiological examination of the compound muscle action potential and sensory nerve action potential as part of the CMT neuropathy score and 10-m Walking Test, Nine-peg-hole Test, Visual Analogue Score (VAS) as well as the dynamometry of single muscles or muscle groups. In our cohort, the mean time of the 10-m Walking Test was 6.1 s (SD = 3.3) and the Nine-peg-hole Test took 27.3 s (SD = 18.9) on average. We measured an average pinch grip of 31.2 N (SD = 24.8) and a mean of the foot dorsiflexion of 19.7 N (SD = 21.9).

$P_{adj} = 0.0072$. Also, age was found to be significant after correction of the *P*-value ($P_{adj} = 0.0465$). In contrast, the marker *CTSA* displayed only borderline significance when the adjusted *P*-value is used ($P_{adj} = 0.0649$). As indicated in the statistical report (Supplementary material), adjusted *P*-values were not calculated for the subcategories of sensory and motor symptoms as no model optimization based on stepwise linear regression was performed for these target variables. The *P*-values show that the model selected for CMT neuropathy score fits well for both subcategories. The 'age' variable had a stronger influence on motor symptoms while *GSTT2* had a stronger correlation with sensory symptoms. The estimated regression coefficients ('Estimate' in Table 5) indicate the size of the predicted change of the dependent target variable if the corresponding independent variable changes by one unit while the other independent variables in the model are kept constant (e.g. the CMT neuropathy score changes 0.159 points if the age is changed by 1 year).

Taken together, by combination of cutaneous expression of *GSTT2* and *CTSA* messenger RNA and age, the model predicts the CMT neuropathy score with an R^2-value of 0.47, indicating that ~47% of total variance of the CMT neuropathy score-related disease severity can be explained by this model (Fig. 4A). The R^2 values for models of motor symptoms and sensory symptoms are both 0.41 (Fig. 4B and C). The expression of a further candidate gene, *PPARG*, shows a significant correlation only with a secondary clinical outcome measure, the 10-m Walking Test ($P = 0.0019$, Fig. 4D). The tested CMT rat disease marker insulin-like growth factor binding protein 5 (*IGFBP5*) and carbonic anhydrase 3 (*CA3*) messenger RNAs revealed no influential values to the CMT neuropathy score-related models. All validated biomarkers in CMT rats and patients with CMT subtype 1A are summarized in Table 6.

Discussion

The factors that determine the interindividual clinical variability and the course of disease in patients with CMT subtype 1A are poorly understood. In the present study, we utilized the disease variability of the CMT rat model to identify messenger RNA transcripts from sciatic nerve and skin biopsies that may serve as biomarkers of disease severity. More specifically, we identified prognostic markers, genes whose expression levels at young age (Day 7) predict clinical impairments at later age (Day 63). We also identified surrogate markers of disease severity at the age of 9 weeks (Day 63). Gene products involved in lipid metabolism were most obviously differentially regulated in sciatic nerve. Importantly, in a direct translational approach, we were able to validate cutaneous disease severity biomarker transcripts in patients with CMT subtype 1A.

Expression of biomarkers in sciatic nerve of Charcot–Marie–Tooth rats

Genes related to lipid metabolism were predominantly downregulated in sciatic nerve tissue of CMT rats when compared with controls at Day 7 as well as at the age of 9 weeks (Day 63) (Fig. 2B). These findings are in accordance with previous observations (Giambonini-Brugnoli *et al.*, 2005; Vigo *et al.*, 2005) and can be regarded as secondary transcriptional response of Schwann cells to the demyelinating pathology. That severely affected CMT rats show a more pronounced downregulation of these genes compared with mildly affected CMT rats at Day 63 (Table 3) may thus also reflect the increased amount of demyelination and axonal loss (Fig. 1E and F; Sereda *et al.*, 2003).

We chose to examine transcriptional expression at the time point Day 7, as there was no phenotype visible and the number of myelinated axons was unaltered in CMT rats when compared with wild-type controls (data not shown). This was thought to relate to time points in young patients with CMT subtype 1A who have not yet developed a clinical phenotype, but who had received a positive genetic analysis. In contrast to Day 63, the validated prognostic marker transcripts of lipid metabolism were upregulated in sciatic nerve tissue in CMT rats, which developed a severe phenotype at later disease stages (Fig. 2B and C; Table 3). Why are the expression levels inversely regulated at early versus late time points? In this regard, we note that 2 days earlier in development (at Day 5) the majority of myelinated axons in sciatic nerve from CMT rats were hypermyelinated (Supplementary Fig. 3), indicating that CMT subtype 1A is a dysmyelinating disease, a notion that is being discussed in spite of the early slowing of nerve conduction velocity in young patients with CMT subtype 1A (Yiu *et al.*, 2008). Hence, increased myelin synthesis may have caused upregulation of lipid genes in CMT rats with severe disease progression at Day 7. We cannot, however, state that the degree of hypermyelination (i.e. increased myelin wraps per axon leading

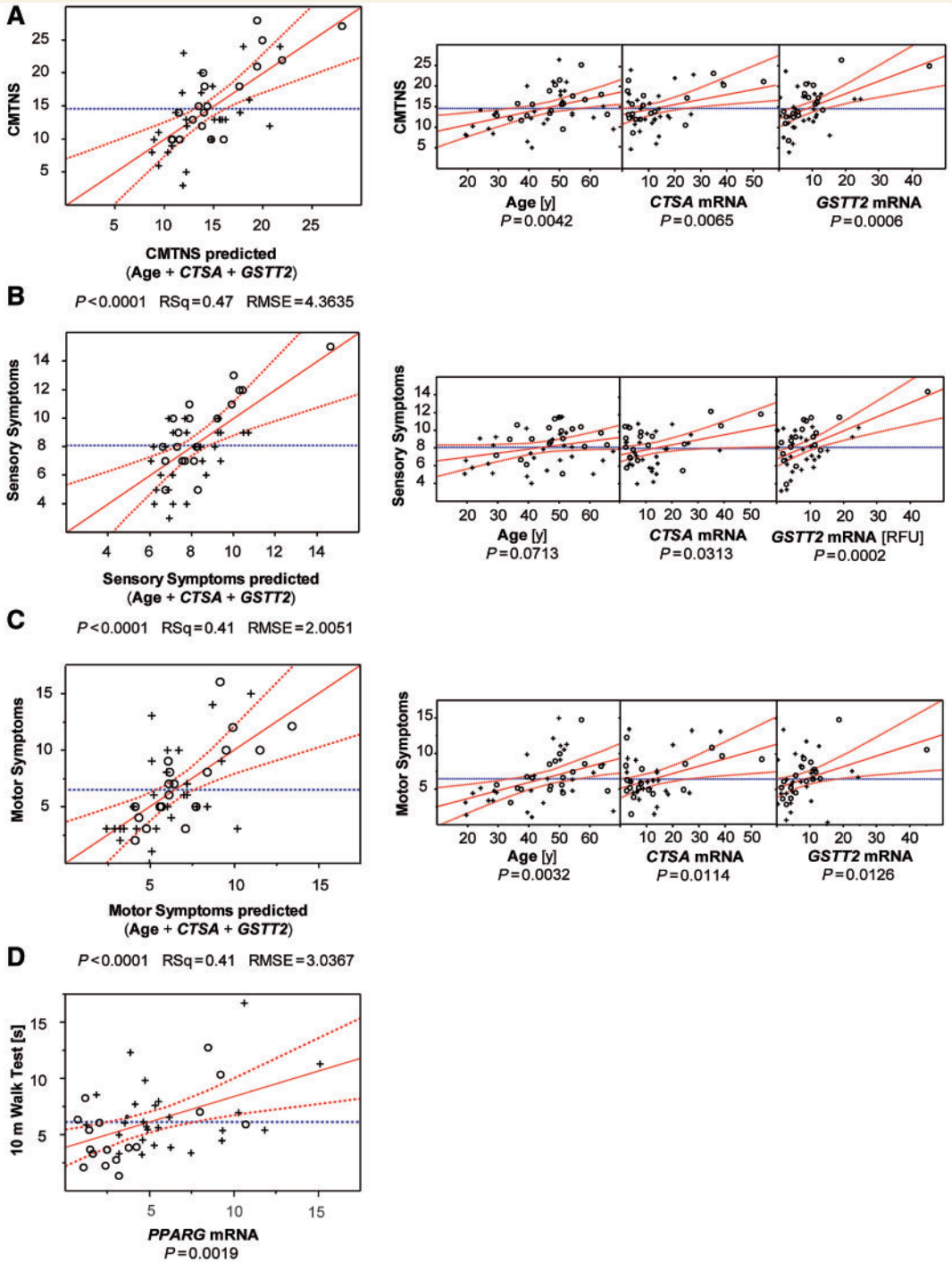

Figure 4 Marker validation in patients with CMT subtype 1A. We examined the clinical variability of 46 genetically determined patients with CMT subtype 1A (+ = female, $n = 27$; o = male, $n = 19$) by applying the CMT neuropathy score (CMTNS) and performed a skin biopsy for subsequent real time-polymerase chain reaction analysis for validation of putative disease markers. Exploratory statistical linear regression modelling was used to identify predictive markers and variables for CMT neuropathy score. (**A**) The variables of the resulting models (*GSTT2* messenger RNA, *CTSA* messenger RNA and age) were used in addition to model the CMT neuropathy score subcategories of sensory symptoms (**B**) and motor symptoms (**C**). The individual contribution of single marker parameters are plotted in leverage graphs next to the CMT neuropathy score-related models. Additionally, cutaneous *PPARG* messenger RNA expression shows significant correlation with the 10-m Walking Test (**D**).

Table 5 Disease severity markers in patients with CMT subtype 1A

Model/dependent variable	Term	Estimate	Standard error	*t*-value	*P*-value	*P*-value adjusted
CMT neuropathy score	Age	0.159	0.052	3.03	0.0042	0.0465
	CTSA	0.161	0.056	2.87	0.0065	0.0649
	GSTT2	0.309	0.083	3.71	0.0006	0.0072
Sensory symptoms	Age	0.046	0.024	1.85	0.0713	n.a.
	CTSA	0.058	0.026	2.23	0.0313	n.a.
	GSTT2	0.158	0.038	4.14	0.0002	n.a.
Motor symptoms	Age	0.114	0.036	3.13	0.0032	n.a.
	CTSA	0.104	0.039	2.65	0.0114	n.a.
	GSTT2	0.151	0.058	2.61	0.0126	n.a.
10-m Walk Test	*PPARG*	0.453	0.136	3.32	0.0019	n.a.

Potentially predictive markers/parameters for CMT neuropathy score should have an adjusted *P*-value (*right*) below the standard alpha level of 0.05. This is true in the CMT neuropathy score model for the marker GSTT2 and for age; the marker CTSA is only borderline significant if the adjusted *P*-value is used. No adjusted *P*-values were calculated for the subcategories of sensory and motor symptoms as no model optimization based on stepwise linear regression had been done for these target variables. The estimated regression coefficients ('Estimate' column) indicate the size of the predicted change of the target variable if the corresponding independent variable changes by one unit while the other independent variables in the model are kept constant. The fourth column gives the standard error of the estimate. The *t*-value in the fifth column is the ratio of Estimate and its standard error. The well known *P*-value can be calculated from the *t*-value and the number of degrees of freedom. n.a. = not analysed.

Table 6 Summary of candidate biomarkers in CMT rats and patients with CMT subtype 1A

Messenger RNA	Prognostic markers		Disease severity markers		
	CMT rats Day 7		CMT rats Day 63		Patients with CMT subtype 1A
	Sciatic nerve	Skin	Sciatic nerve	Skin	Skin
Pparg	↑	–	↓	↑	↑
Lpl	↑	–	↓	–	n.a.
Thrsp	↑	–	↓	–	n.a.
Gstt2	–	↑	–	↑	↑
Ctsa	–	↑	–	↑	↑
Pmp22	–	↑	–	–	n.a.

Validation of selected prognostic (Day 7) and disease severity markers (Day 63) in the CMT rat and in patients with CMT subtype 1A. Arrows indicate up- or downregulation in severely affected CMT rats and patients with CMT subtype 1A. Minus sign indicates no regulation, whereas n.a. denotes not analysed.

to a lower *g*-ratio) at Day 7 directly predisposes to increased axonal loss at later time points. Nevertheless, it is tempting to speculate that early dysregulation of lipid metabolism associated genes triggered by *Pmp22* overexpression may cause more severe axonal loss and a clinical phenotype in CMT subtype 1A as lipids constitute ~70% of total myelin and lipid metabolism plays an important role in myelination and demyelination (Garbay *et al.*, 2000; Saher *et al.*, 2009). Further focus on the role of PMP22 with regard to lipid metabolism in the CMT subtype 1A disease pathology will elucidate this question. Interestingly, sciatic nerve *Pmp22* messenger RNA expression itself did not contribute to disease severity at Day 7 and Day 63 (Table 3).

Pparg, *Lpl* and *Thrsp* messenger RNAs are examples of lipid metabolism-related, differentially regulated genes at both time points, Day 7 and Day 63, in the sciatic nerve of CMT rats (Fig. 2D). These genes may therefore indicate disease progression modifiers. *Pparg* messenger RNA was also identified as a disease severity marker in skin of CMT rats at Day 63 (Fig. 3C). In patients with CMT subtype 1A, the cutaneous expression of *PPARG* shows significant correlation with the 10-m Walking Test, a secondary motor outcome measure (Fig. 4D), which makes it a particularly interesting gene with regard to CMT subtype 1A pathology. PPARG protein is a lipid-activated member of the nuclear receptor superfamily of transcription factors and controls the expression of a battery of genes involved in lipid metabolism (reviewed in Tontonoz and Spiegelmann, 2008). With regard to the PNS, two reports indicate that PPARG ligands can reduce neuropathic pain in animal models of sciatic nerve injury (Seltzer *et al.*, 1990; Maeda *et al.*, 2008). After spinal cord injury, application of PPARG agonists can prevent motor dysfunction and myelin loss in the CNS of adult rats (Park *et al.*, 2007). Treatment with agonistic PPARG ligands may therefore constitute a future therapeutic rational in CMT subtype 1A.

Expression of biomarkers in skin biopsies of Charcot–Marie–Tooth rats

Nerve biopsies constitute an important, but invasive diagnostic tool. In the more easily accessible cutaneous tissue of patients with CMT subtype 1A and different animal models of hereditary neuropathies, pathologically demyelinated axons as well as altered myelin gene expression in subcutaneous nerve bundles could be identified (Fig. 3A; Li *et al.*, 2005; Meyer zu Hörste *et al.*, 2007;

Dacci *et al.*, 2010). With regard to the powerful translational aspect of skin biopsies in patients (Lauria *et al.*, 2011) we therefore determined whether biomarkers could be identified from skin biopsies in CMT rats.

In general, the expression of candidate biomarker transcripts highly differed between sciatic nerve and skin (Tables 3 and 6). Which cells contribute to the expression of genes in skin? Despite the presence of myelinated nerve fibres in the subcutaneous layer of skin tissue (Fig. 3A), a predominant contribution of Schwann cell-derived messenger RNA to the entire dermal transcriptome is very unlikely given the vast majority of dermal cells such as fibroblasts and keratinocytes (Kanitakis, 2002).

The altered gene expression observed in skin biopsies may reflect loss of axons and sensory effector organs in skin tissue (Saporta *et al.*, 2009). Alternatively, skin derived fibroblasts and keratinocytes may be subjected to secondary remodelling processes of subcutaneous and cutaneous tissue as a consequence of the atrophy of the small finger muscles, a described early and sensitive feature of patients with CMT subtype 1A (Berciano *et al.*, 2000). Thus, the altered gene expression profile from cutaneous tissue may be seen as a sensitive surrogate marker of axonal loss and consecutive muscle atrophy.

In our transcriptional analysis of dermal tissue we validated six genes at Day 7, which constitute prognostic markers from skin biopsies in the CMT rat model (Table 3). Importantly, *Pmp22* was the most robust identified cutaneous prognostic marker, since CMT rats with moderate disease progression already showed a significant upregulation when compared with wild-type controls at Day 7 (Fig. 3C).

Ctsa and *Gstt2* were identified as prognostic and disease severity markers in skin of the CMT rat. Moreover, we demonstrate that the dermal messenger RNA expression of *Gstt2* also correlates with the phenotype of CMT rats after an experimental therapeutic approach with a progesterone antagonist, which we had performed in an earlier study (Supplementary Fig. 2; Meyer zu Hörste *et al.*, 2007), indicating that *Gstt2* may be a promising cutaneous disease severity marker for monitoring future therapeutic trials in patients (Supplementary Fig. 2).

Validation of biomarkers in skin biopsies of patients with Charcot–Marie–Tooth subtype 1A

In a cohort of 46 patients with CMT subtype 1A, we show significant correlations between the CMT neuropathy score and its subcategories (sensory and motor symptoms), with the dermal messenger RNA expressions of *GSTT2* and *CTSA* (Fig. 4A–C). We could also confirm previous findings (Shy *et al.*, 2008), that the age of patients with CMT subtype 1A correlates with disease severity. Importantly, by combination of the variables *GSTT2* and *CTSA* messenger RNA and age, the surrogate marker value for the CMT neuropathy score shows an R^2 of 0.47 (47%) (Fig. 4A). The R^2 values for the models 'motor symptoms' and 'sensory symptoms' are both 0.41 (41%) (Fig. 4B and C). The effect sizes of 47% and 41% can be interpreted as 'moderate to strong' under classical statistical criteria (Cohen, 1988; Evans, 1996).

The major limitations of these results are that the models in the statistical analysis are data derived and not preplanned. The development of applicable biomarkers necessitates extensive evaluation in larger studies with explicit, criterion-based, quantitative and multidimensional hierarchical levels of evidence schema (Lassere, 2008; Pletcher and Pignone, 2011). However, the statistical models with formally significant predictors in our study can be considered as appropriate to generate promising hypotheses (Supplementary material). Our data demonstrate that—in principle—disease severity can be correlated with cutaneous messenger RNA expression in the CMT rat and in patients affected with CMT subtype 1A. Currently, we are performing a larger confirmative study to challenge all identified rodent biomarkers in patients with CMT subtype 1A on newly captured data. We aim to provide clinicians with applicable biomarkers which may find implementation in future therapy trials.

The statistical analysis of the present human data was performed regardless of potentially perturbing influential factors such as sex, medications, comorbidities and other risk factors. Although environmental factors can be assumed to influence CMT disease severity, we observed a marked interindividual variability in disease severity in CMT rats that were kept on an outbred background under identical conditions. Therefore, in CMT rats, we speculate that environmental factors can be largely excluded to have caused disease variability, indicating that intrinsic genetic factors suffice to entail differential disease progression.

Importantly, three of five tested CMT rat-derived cutaneous disease severity markers showed an influence on the CMT neuropathy score-related models of patients with CMT subtype 1A. We conclude that the transcriptional regulation in skin tissue with regard to disease severity is similar when comparing CMT rats and patients with CMT subtype 1A. Finally, the approach in this study may reflect a practical approach to identify modifying genes, rather than using genome-wide searching (Genin *et al.*, 2008).

Acknowledgements

We thank C. Stünkel for excellent technical assistance and M. Wehe for excellent animal care. We are grateful to members of the Nave lab for discussion.

Funding

R.F., B.S.-W., U.H. and M.W.S. were supported by the German Ministry of Education and Research (BMBF, FKZ: 01ES0812 to M.W.S., M.J.R. and B.R.). This study was supported in part by the Association Francaise contre Les Myopathies (AFM, Nr: 15037 to M.W.S.).

Supplementary material

Supplementary material is available at *Brain* online.

References

Bannon AW, Malmberg AB. Models of nociception: hot-plate, tail-flick, and formalin tests in rodents. Curr Protoc Neurosci 2007; Chapter 8: Unit 8 9.

Berciano J, Garcia A, Calleja J, Combarros O. Clinico-electrophysiological correlation of extensor digitorum brevis muscle atrophy in children with charcot-marie-tooth disease 1A duplication. Neuromuscul Disord 2000; 10: 419–24.

Burns J, Ouvrier RA, Yiu EM, Joseph PD, Kornberg AJ, Fahey MC, et al. Ascorbic acid for Charcot-Marie-Tooth disease type 1A in children: a randomised, double-blind, placebo-controlled, safety and efficacy trial. Lancet Neurol 2009; 8: 537–44.

Cohen J. Statistical power analysis for the behavioral sciences. 2nd edn. Hillsdale, NJ: L. Erlbaum Associates; 1988.

Dacci P, Dina G, Cerri F, Previtali SC, Lopez ID, Lauria G, et al. Foot pad skin biopsy in mouse models of hereditary neuropathy. Glia 58: 2005–16.

de Visser M, Verhamme C. Ascorbic acid for treatment in CMT1A: what's next? Lancet Neurol10: 291–3.

Evans JD. Straightforward statistics for the behavioral sciences. Pacific Grove, CA: Brooks/Cole Pub. Co.; 1996.

Garbay B, Heape AM, Sargueil F, Cassagne C. Myelin synthesis in the peripheral nervous system. Prog Neurobiol 2000; 61: 267–304.

Garcia CA, Malamut RE, England JD, Parry GS, Liu P, Lupski JR. Clinical variability in two pairs of identical twins with the Charcot-Marie-Tooth disease type 1A duplication. Neurology 1995; 45: 2090–3.

Genin E, Feingold J, Clerget-Darpoux F. Identifying modifier genes of monogenic disease: strategies and difficulties. Hum Genet 2008; 124: 357–68.

Giambonini-Brugnoli G, Buchstaller J, Sommer L, Suter U, Mantei N. Distinct disease mechanisms in peripheral neuropathies due to altered peripheral myelin protein 22 gene dosage or a Pmp22 point mutation. Neurobiol Dis 2005; 18: 656–68.

Kaku DA, Parry GJ, Malamut R, Lupski JR, Garcia CA. Nerve conduction studies in Charcot-Marie-Tooth polyneuropathy associated with a segmental duplication of chromosome 17. Neurology 1993; 43: 1806–8.

Kanitakis J. Anatomy, histology and immunohistochemistry of normal human skin. Eur J Dermatol 2002; 12: 390–9; quiz 400–1.

Karlsson U, Schultz RL. Fixation of the central nervous system from electron microscopy by aldehyde perfusion. I. preservation with aldehyde perfusates versus direct perfusion with osmium tetroxide with special reference to membranes and the extracellular space. J Ultrastruct Res 1965; 12: 160–86.

Katona I, Wu X, Feely SM, Sottile S, Siskind CE, Miller LJ, et al. PMP22 expression in dermal nerve myelin from patients with CMT1A. Brain 2009; 132: 1734–40.

Krajewski KM, Lewis RA, Fuerst DR, Turansky C, Hinderer SR, Garbern J, et al. Neurological dysfunction and axonal degeneration in Charcot-Marie-Tooth disease type 1A. Brain 2000; 123 (Pt 7): 1516–27.

Lassere MN. The Biomarker-Surrogacy Evaluation Schema: a review of the biomarker-surrogate literature and a proposal for a criterion-based, quantitative, multidimensional hierarchical levels of evidence schema for evaluating the status of biomarkers as surrogate endpoints. Stat Methods Med Res 2008; 17: 303–40.

Lauria G, Cazzato D, Porretta-Serapiglia C, Casanova-Molla J, Taiana M, Penza P, et al. Morphometry of dermal nerve fibers in human skin. Neurology 2011; 77: 242–9.

Li J, Bai Y, Ghandour K, Qin P, Grandis M, Trostinskaia A, et al. Skin biopsies in myelin-related neuropathies: bringing molecular pathology to the bedside. Brain 2005; 128: 1168–77.

Luft JH. Improvements in epoxy resin embedding methods. J Biophys Biochem Cytol 1961; 9: 409–14.

Lupski JR, de Oca-Luna RM, Slaugenhaupt S, Pentao L, Guzzetta V, Trask BJ, et al. DNA duplication associated with Charcot-Marie-Tooth disease type 1A. Cell 1991; 66: 219–32.

Maeda T, Kiguchi N, Kobayashi Y, Ozaki M, Kishioka S. Pioglitazone attenuates tactile allodynia and thermal hyperalgesia in mice subjected to peripheral nerve injury. J Pharmacol Sci 2008; 108: 341–7.

Martyn CN, Hughes RA. Epidemiology of peripheral neuropathy. J Neurol Neurosurg Psychiatry 1997; 62: 310–8.

Matsunami N, Smith B, Ballard L, Lensch MW, Robertson M, Albertsen H, et al. Peripheral myelin protein-22 gene maps in the duplication in chromosome 17p11.2 associated with Charcot-Marie-Tooth 1A. Nat Genet 1992; 1: 176–9.

Meyer OA, Tilson HA, Byrd WC, Riley MT. A method for the routine assessment of fore- and hindlimb grip strength of rats and mice. Neurobehav Toxicol 1979; 1: 233–6.

Meyer zu Hörste G, Prukop T, Liebetanz D, Mobius W, Nave KA, Sereda MW. Antiprogesterone therapy uncouples axonal loss from demyelination in a transgenic rat model of CMT1A neuropathy. Ann Neurol 2007; 61: 61–72.

Micallef J, Attarian S, Dubourg O, Gonnaud PM, Hogrel JY, Stojkovic T, et al. Effect of ascorbic acid in patients with Charcot-Marie-Tooth disease type 1A: a multicentre, randomised, double-blind, placebo-controlled trial. Lancet Neurol 2009; 8: 1103–10.

Mootha VK, Lepage P, Miller K, Bunkenborg J, Reich M, Hjerrild M, et al. Identification of a gene causing human cytochrome c oxidase deficiency by integrative genomics. Proc Natl Acad Sci USA 2003; 100: 605–10.

Pareyson D, Marchesi C, Salsano E. Hereditary predominantly motor neuropathies. Curr Opin Neurol 2009; 22: 451–9.

Pareyson D, Reilly MM, Schenone A, Fabrizi GM, Cavallaro T, Santoro L, et al. Ascorbic acid in Charcot-Marie-Tooth disease type 1A (CMT-TRIAAL and CMT-TRAUK): a double-blind randomised trial. Lancet Neurol 2011; 10: 320–8.

Park SW, Yi JH, Miranpuri G, Satriotomo I, Bowen K, Resnick DK, et al. Thiazolidinedione class of peroxisome proliferator-activated receptor gamma agonists prevents neuronal damage, motor dysfunction, myelin loss, neuropathic pain, and inflammation after spinal cord injury in adult rats. J Pharmacol Exp Ther 2007; 320: 1002–12.

Parman Y. Hereditary neuropathies. Curr Opin Neurol 2007; 20: 542–7.

Patel PI, Roa BB, Welcher AA, Schoener-Scott R, Trask BJ, Pentao L, et al. The gene for the peripheral myelin protein PMP-22 is a candidate for Charcot-Marie-Tooth disease type 1A. Nat Genet 1992; 1: 159–65.

Pletcher MJ, Pignone M. Evaluating the clinical utility of a biomarker: a review of methods for estimating health impact. Circulation 123: 1116–24.

Raeymaekers P, Timmerman V, Nelis E, De Jonghe P, Hoogendijk JE, Baas F, et al. Duplication in chromosome 17p11.2 in Charcot-Marie-Tooth neuropathy type 1a (CMT 1a). The HMSN Collaborative Research Group. Neuromuscul Disord 1991; 1: 93–7.

Reilly MM, de Jonghe P, Pareyson D. 136th ENMC International Workshop: Charcot-Marie-Tooth disease type 1A (CMT1A)8-10 April 2005, Naarden, The Netherlands. Neuromuscul Disord 2006; 16: 396–402.

Reilly MM, Shy ME, Muntoni F, Pareyson D. 168th ENMC International Workshop: outcome measures and clinical trials in Charcot-Marie-Tooth disease (CMT). Neuromuscul Disord 2010; 839–46.

Rossner MJ, Hirrlinger J, Wichert SP, Boehm C, Newrzella D, Hiemisch H, et al. Global transcriptome analysis of genetically identified neurons in the adult cortex. J Neurosci 2006; 26: 9956–66.

Saher G, Quintes S, Mobius W, Wehr MC, Kramer-Albers EM, Brugger B, et al. Cholesterol regulates the endoplasmic reticulum exit of the major membrane protein P0 required for peripheral myelin compaction. J Neurosci 2009; 29: 6094–104.

Saporta MA, Katona I, Lewis RA, Masse S, Shy ME, Li J. Shortened internodal length of dermal myelinated nerve fibres in Charcot-Marie-Tooth disease type 1A. Brain 2009; 132: 3263–73.

Seltzer Z, Dubner R, Shir Y. A novel behavioral model of neuropathic pain disorders produced in rats by partial sciatic nerve injury. Pain 1990; 43: 205–18.

Sereda M, Griffiths I, Puhlhofer A, Stewart H, Rossner MJ, Zimmerman F, et al. A transgenic rat model of Charcot-Marie-Tooth disease. Neuron 1996; 16: 1049–60.

Sereda MW, Meyer zu Hörste G, Suter U, Uzma N, Nave KA. Therapeutic administration of progesterone antagonist in a model of Charcot-Marie-Tooth disease (CMT-1A). Nat Med 2003; 9: 1533–7.

Shy ME, Blake J, Krajewski K, Fuerst DR, Laura M, Hahn AF, et al. Reliability and validity of the CMT neuropathy score as a measure of disability. Neurology 2005a; 64: 1209–14.

Shy ME, Chen L, Swan ER, Taube R, Krajewski KM, Herrmann D, et al. Neuropathy progression in Charcot-Marie-Tooth disease type 1A. Neurology 2008; 70: 378–83.

Shy ME, Lupski JR, Chance PF, Klein CJ, Dyck PJ. Hereditary motor and sensory neuropathies: an overview of clinical, geneti, electrophysiologic, and pathologic features. In: Dyck PJ, Thomas PK, editors. Peripheral neuropathy. Vol. 2. Philadelphia: Elsevier Saunders; 2005b. p. 1623–58.

Skre H. Genetic and clinical aspects of Charcot-Marie-Tooth's disease. Clin Genet 1974; 6: 98–118.

Steiner I, Gotkine M, Steiner-Birmanns B, Biran I, Silverstein S, Abeliovich D, et al. Increased severity over generations of Charcot-Marie-Tooth disease type 1A. J Neurol 2008; 255: 813–9.

Subramanian A, Tamayo P, Mootha VK, Mukherjee S, Ebert BL, Gillette MA, et al. Gene set enrichment analysis: a knowledge-based approach for interpreting genome-wide expression profiles. Proc Natl Acad Sci USA 2005; 102: 15545–50.

Thomas PK, Marques W Jr, Davis MB, Sweeney MG, King RH, Bradley JL, et al. The phenotypic manifestations of chromosome 17p11.2 duplication. Brain 1997; 120 (Pt 3): 465–78.

Timmerman V, Nelis E, Van Hul W, Nieuwenhuijsen BW, Chen KL, Wang S, et al. The peripheral myelin protein gene PMP-22 is contained within the Charcot-Marie-Tooth disease type 1A duplication. Nat Genet 1992; 1: 171–5.

Tontonoz P, Spiegelman BM. Fat and beyond: the diverse biology of PPARgamma. Annu Rev Biochem 2008; 77: 289–312.

Valentijn LJ, Bolhuis PA, Zorn I, Hoogendijk JE, van den Bosch N, Hensels GW, et al. The peripheral myelin gene PMP-22/GAS-3 is duplicated in Charcot-Marie-Tooth disease type 1A. Nat Genet 1992; 1: 166–70.

Vandesompele J, De Preter K, Pattyn F, Poppe B, Van Roy N, De Paepe A, et al. Accurate normalization of real-time quantitative RT-PCR data by geometric averaging of multiple internal control genes. Genome Biol 2002; 3: RESEARCH0034.

Verhamme C, de Haan RJ, Vermeulen M, Baas F, de Visser M, van Schaik IN. Oral high dose ascorbic acid treatment for one year in young CMT1A patients: a randomised, double-blind, placebo-controlled phase II trial. BMC Med 2009; 7: 70.

Vigo T, Nobbio L, Hummelen PV, Abbruzzese M, Mancardi G, Verpoorten N, et al. Experimental Charcot-Marie-Tooth type 1A: a cDNA microarrays analysis. Mol Cell Neurosci 2005; 28: 703–14.

Yiu EM, Burns J, Ryan MM, Ouvrier RA. Neurophysiologic abnormalities in children with Charcot-Marie-Tooth disease type 1A. J Peripher Nerv Syst 2008; 13: 236–41.

Young P, De Jonghe P, Stogbauer F, Butterfass-Bahloul T. Treatment for Charcot-Marie-Tooth disease. Cochrane Database Syst Rev 2008; CD006052.